

Overview and developments for the Phase-II upgrade of the inner tracker of the ATLAS experiment

Helen Hayward^{*†}

University of Liverpool (UK)

E-mail: helen.hayward@cern.ch

In the high luminosity era of the Large Hadron Collider (HL-LHC), the instantaneous luminosity is expected to reach unprecedented values, resulting in about 200 proton-proton interactions in a typical bunch crossing. To cope with the resultant increase in occupancy, bandwidth and radiation damage, the ATLAS Inner Detector will be replaced by an all-silicon system, the Inner Tracker (ITk), aiming to provide tracking coverage up to $|\eta| < 4$.

The ITk consists of an inner pixel and an outer strip detector. The total surface area of silicon in the new pixel system could measure up to 14 m², depending on the final layout choice, due in 2017. The strip detector will comprise up to 190 m² of silicon. In the collaboration a large effort is ongoing to evaluate the design both with simulation and experimental results. In this report, highlight results of various components like sensors, modules and larger structures for both the pixel and strip detector are shown.

The European Physical Society Conference on High Energy Physics

5-12 July

Venice, Italy

^{*}Speaker.

[†]On behalf of the ATLAS ITk Collaboration

1. Introduction

A replacement tracking detector is currently being designed for the ATLAS experiment for the start of the High-Luminosity LHC (HL-LHC) in 2026. The HL-LHC has a design peak instantaneous luminosity of $\mathcal{L} = 7.5 \times 10^{34} \text{ cm}^{-2}\text{s}^{-1}$, corresponding to approximately 200 inelastic proton-proton collisions per beam crossing, and ATLAS is expected to collect an integrated luminosity of up to 4000 fb^{-1} over approximately 10 years. For contrast, the current LHC is operating with a peak number of interactions per bunch crossing of 40, and ATLAS is expected to collect 300 fb^{-1} before 2023. A new tracker detector is required due to the expected radiation damage, bandwidth saturation and limitations from detector occupancy from the HL-LHC.

The Inner TrackER (ITk) comprises of an inner pixel and outer strip detector, both composed of barrel and endcap regions, providing an $|\eta|$ coverage up to 4, as shown in Figure 1. It has been designed on the basis that it should provide the same tracking performance as the current tracker detector, but in the harsher environment of the HL-LHC [1].

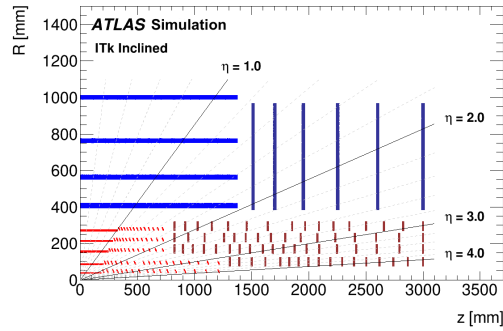


Figure 1: A quarter-section $r - z$ view of the ATLAS ITk tracker presented in the Strip Technical Design Report [1] showing the coverage of the pixel detector in red and strip detector in blue.

2. Strip Detector

There are eight types of strip sensor, two for the barrel, and six in the endcap. For the barrel, modules either have four rows of short strips (24.10 mm in length) or two rows of long strips (48.20 mm in length). There are six different shape strip sensors in the endcap to cover each strip petal, the main structure comprising each endcap disk (see Figure 2). Each strip module side consists of one sensor and one or two low-mass printed circuit boards, called hybrids, hosting the read-out application-specific integrated circuits (ASICs). Modules have been designed with mass production and low cost in consideration. The strips are AC-coupled with n-type implants in a p-type float-zone silicon bulk (known as n+-in-p FZ). The choice of using n+-in-p technology, over the p-in-n used in the current strip tracker detector, is the large difference in the amount of signal after irradiation.

An exploded view of a short-strip module is shown in Figure 3. Figure 4 illustrates the performance of prototype sensors for the long-strip (LS) module. The left plot shows the charge collection as a function of fluence is fairly consistent for a variety of modules irradiated with different energy particles, with the charge collection reducing as the fluence increases. As the charge

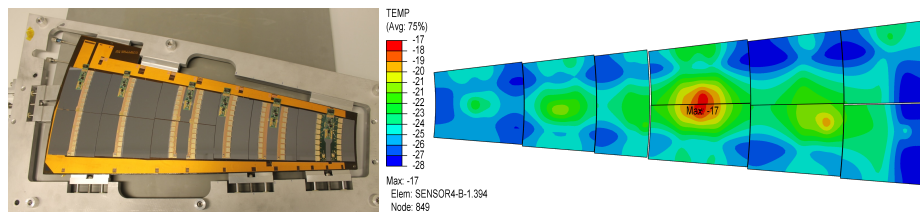


Figure 2: Left: Photo of the thermo-mechanical petal prototype. Right: Temperature distribution within the FEA model, given the estimated power consumption after 3000 fb^{-1} [1].

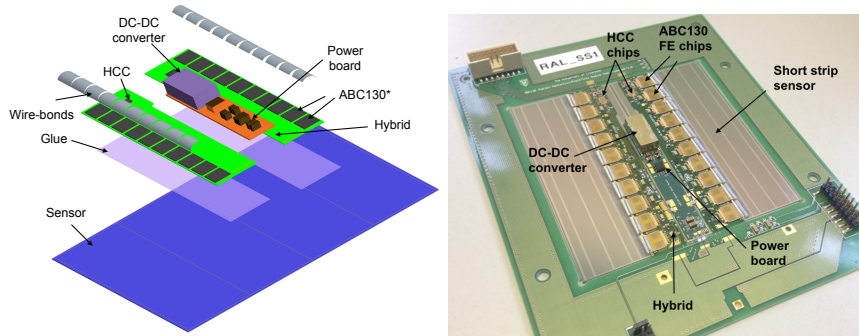


Figure 3: Left: Exploded view of a short-strip barrel module with all relevant components. Right: Fully assembled short-strip barrel module with ATLAS12 sensor and ABC130 chips including power board [1].

collection reduces, the efficiency of the module decreases. This is shown in the right plot which shows the efficiency of radiated and irradiated sensors, as a function of threshold, when placed in a test beam at CERN.

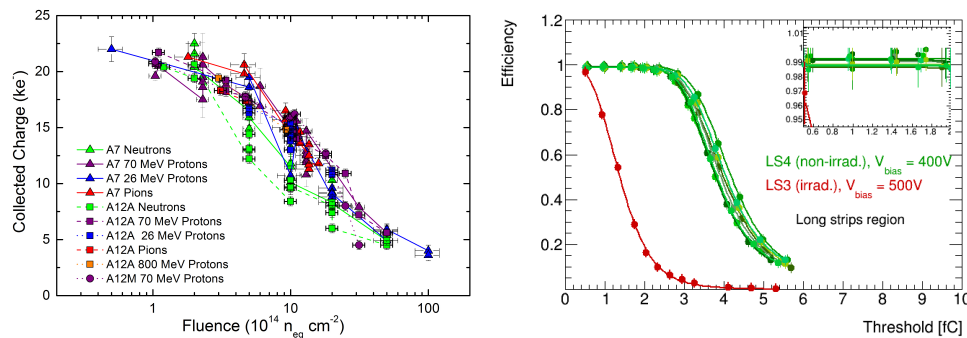


Figure 4: Left: Collected signal charge at 500 V bias voltage for minimum ionising particles as a function of $1 \text{ MeV } n_{\text{eq}}/\text{cm}^2$ fluence for various types of particles [3]. The vertical dashed line indicates the maximal expected fluence within the ITk Strip Detector (incl. safety factor). Right: The efficiency versus the threshold for four ASICs on the non-irradiated module LS4 (shown in green), and one ASIC on the irradiated module LS3 (shown in red) [1].

In addition to performance studies of sensors and modules, prototypes of the larger mechanical structures have been tested. Figure 2 shows studies a photo of a thermo-mechanical petal prototype, along with the stable temperature solution predicted from the finite-element-model (FEA), at the maximum expected sensor power. This is crucial to establish the design of the petal and its cooling

protects it from thermal runaway. Figure 5 shows a mechanical model of the support structure for the endcap petals including the services modules together with the gravitational sag as predicted by the FEA. The maximum sag is $70 \mu\text{m}$ which is within the specifications required.

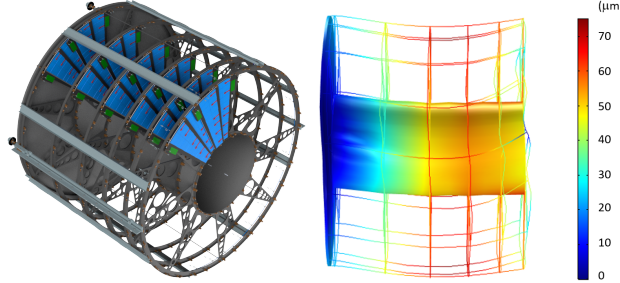


Figure 5: Left: An end-cap service module serving. Each service module electrically serve a section in ϕ comprising four petals in each disk. Right: Results of the gravitational sag analysis [1].

3. Pixel Detector

The baseline pixel module is a hybrid pixel detector composed of a sensor and the read-out chip (ROIC) bump bonded to each other on a pixel level. There are two types of these modules: quad modules ($4 \times 4 \text{ cm}^2$) and dual modules ($2 \times 4 \text{ cm}^2$) with 4 and 2 chips respectively. Prototypes are based on the previous ATLAS pixel read-out chip FE-I4 (with dimensions $50 \times 250 \mu\text{m}^2$) whilst the final readout chip is currently under development within the RD53 collaboration [2]. The RD53 chip ($50 \times 50 \mu\text{m}^2$) will then lead to the final ATLAS ITk pixel chip with additional functionality based on the ATLAS specifications. The RD53 module utilises n-in-p compared to current n-in-n electrode arrangement and a reduced thickness of $100\text{-}150 \mu\text{m}$ (currently $200 \mu\text{m}$). A prototype of the quad-module with four FE-I4 chips is presented in Figure 6, together with the number of hits recorded per pixel, of the prototype, to ^{241}Am gamma radiation. Prototype modules have been irradiated with different fluences to fully study the behaviour inside an operating detector. Figure 7(left) shows a comparison of hit efficiencies for different thickness sensors, demonstrating the thinner $100 \mu\text{m}$ sensor can provide the same efficiency at lower bias voltages than the thicker sensors. Figure 7(right) shows how the efficiency decreases as the irradiation of the planar sensors increases but still remains adequate at the expected integrated dose.

Two other sensor technologies are under consideration for the pixel sensors. 3D pixel detectors are currently used for the Inner B-layer for the current detector, and are candidates for the innermost layers of the ITk due to their good radiation hardness at low operational voltages and moderate temperatures and low power dissipation. Prototype 3D sensors used with the FE-I4 chip have been produced and extensively tested before and after radiation. Figure 8(left) shows the hit efficiency as a function of bias voltage for difference fluences (Φ), thresholds and tilts. It can be seen that the efficiency falls as the threshold increases, the fluence increases or the tilt angle decreases.

CMOS pixel sensors are under consideration for the outer pixel layers. These typically have a sensing substrate and a CMOS electronics layer embedded in multiple cells. They are a promising technology, commonly used in industry, that would reduce costs whilst providing high granularity, radiation hard sensors for outer pixel layers, being able to withstand radiation fluences $> 5 \times$

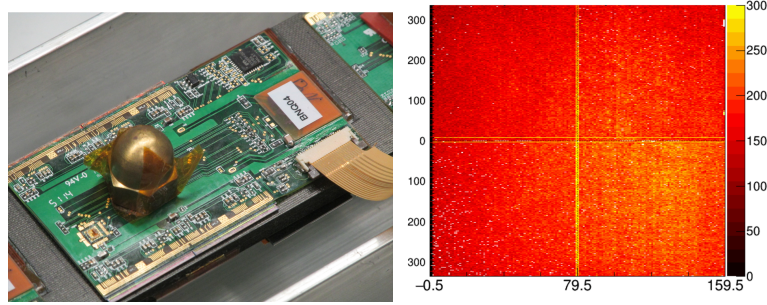


Figure 6: Left: Prototype of the quad-module with four FE-I4 chips. The metal cup shown is for protection of the chip on the hybrid for serial powering control. Right: The number of hits recorded per pixel in response to ^{241}Am gamma radiation of a quad module prototype. The high hit pixels are due to their larger size in the inter-chip region [1].

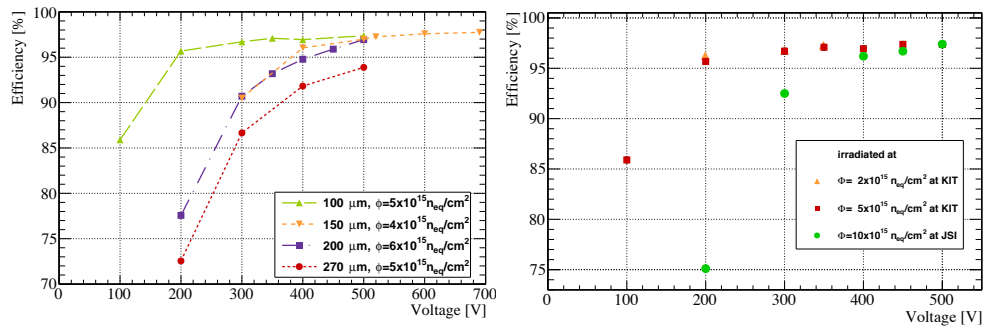


Figure 7: Left: Comparison of hit efficiencies, for different thickness planar sensors as a function of bias voltage, after a fluence of approximately $5 \times 10^{15} \text{ n}_{\text{eq}}/\text{cm}^2$. Right: Comparison of hit efficiencies of FE-I4 modules with $100 \mu\text{m}$ thin planar sensors irradiated from a fluence of $2 \times 10^{15} \text{ n}_{\text{eq}}/\text{cm}^2$ to $10^{16} \text{ n}_{\text{eq}}/\text{cm}^2$ [1].

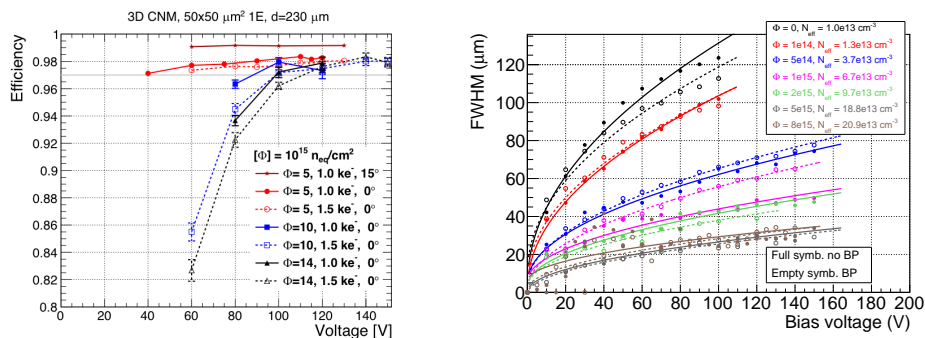


Figure 8: Left: Efficiency as a function of bias voltage for prototype 3D sensors with different fluences, thresholds and tilts [4]. Right : Collection width for CMOS Pixel sensor (LFoundry) after irradiation [1].

$10^{15} \text{ n}_{\text{eq}}/\text{cm}^2$. Figure 8(right) shows the collection width (measured at full width at half maximum, FWHM) of the order of a few $10 \mu\text{m}$ can be obtained for non-irradiated and irradiated sensors of different tilt angles and fluence.

Prototypes have been developed for different possible designs for the local supports of the pixel detector. As an example, Figure 9 shows the truss prototype for longeron design for outer pixel barrel together with a sketch of the completed structure.

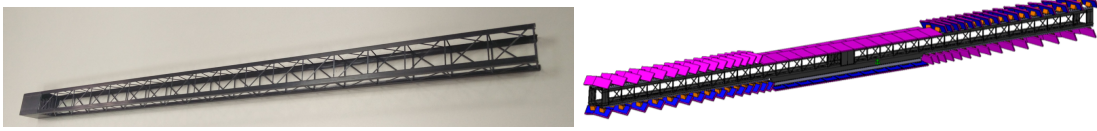


Figure 9: Prototype truss (left) and sketch (right) of longeron design for outer pixel barrel.

4. Resulting ITK material budget and conclusions

The work to reduce the material by careful choice of pixel and strip module designs and support structure has resulted in a design for the ITk with an estimated budget of around 30% lower in the region $|\eta| < 4.0$, compared to the Run 2 detector. The estimated fluence distribution for the ITk after 3000 fb^{-1} is presented in Figure 10(left). This plot shows that the maximum 1 MeV neutron equivalent fluences for the pixels and strip detectors are predicted to be 1.5×10^{16} and $8.2 \times 10^{14} \text{ n}_{\text{eq}}/\text{cm}^2$, which is less than the maximum allowed fluence (including safety factors) of 1.87×10^{16} and $1.2 \times 10^{15} \text{ n}_{\text{eq}}/\text{cm}^2$ respectively [1]. This low mass detector has an estimated distribution in radiation lengths of material as a function of η shown in in Figure 10(right).

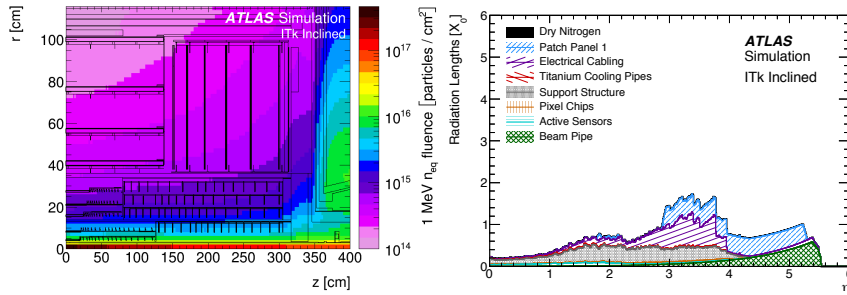


Figure 10: Left: The estimated fluence distribution for the ITk after 3000 fb^{-1} . Right: Radiation length as a function of $|\eta|$ for the ITk [1].

References

- [1] The ATLAS Collaboration, CERN-LHCC-2017-005, ATLAS-TDR-025.
- [2] <http://www.cern.ch/RD53>.
- [3] K. Hara *et al.*, Nucl. Instrum. Meth. A **831** (2016) 181. doi:10.1016/j.nima.2016.04.035
- [4] J. Lange *et al.*, TIPP 2017 Proceedings, arXiv:1707.01045.